sustainability

MDPI

Article

Rapid Retrofit of Reinforced Concrete Frames after Progressive Collapse to Increase Sustainability

Shuang Li [1], Sidi Shan [2,*], Haiyu Zhang [1] and Yi Li [3]

1 Key Lab of Structures Dynamic Behavior and Control of the Ministry of Education, Key Lab of Smart Prevention and Mitigation of Civil Engineering Disasters of the Ministry of Industry and Information Technology, Harbin Institute of Technology, Harbin 150090, China
2 School of Resources and Civil Engineering, Northeastern University, Shenyang 110819, China
3 The Key Laboratory of Urban Security and Disaster Engineering, Ministry of Education, Beijing University of Technology, Beijing 100124, China
* Correspondence: shansidi@mail.neu.edu.cn; Tel.: +86-451-8628-2095

Received: 11 June 2019; Accepted: 16 July 2019; Published: 2 August 2019

check for updates

Abstract: A structural progressive collapse is usually a local failure, in which the damage is concentrated at beams that bridge the removal column and the column itself. In many cases, retrofitting the damaged structure is more economical and more sustainable than reconstructing the entire structure. A progressive collapse test of a 1/3 scale, four-bay by two-story reinforced concrete (RC) frame was conducted, after which the structure was retrofitted with carbon fiber reinforced polymer (CFRP) wraps and retested. The center column in the first story was removed and the frame was pushed down quasistatically under displacement control to investigate the progressive collapse performances of the retrofitted RC frame. The test results were represented systematically at different areas in terms of the resistance forces, crack developments, and local and global failure modes. Numerical models were built to verify the test frame before and after the retrofitting. A design method was proposed to retrofit an RC frame using CFRP wraps after a progressive collapse. The test frame was redesigned to improve the retrofitting and used as an example to demonstrate the rationality of the proposed retrofit design method. The results indicated that the proposed retrofitting technology rapidly restored the frame structure to its original capacity before the progressive collapse occurred, whilst consistently satisfying the priorities of being economical and sustainable.

Keywords: RC frame; CFRP wraps; progressive collapse; rapid retrofit; sustainability

1. Introduction

Progressive collapse is a phenomenon involving the spread of an initial local failure from element to element, eventually resulting in the collapse of an entire structure or a disproportionately large part of a structure, which can be induced by accidental loads [1,2]. Progressive collapse is a relatively rare event, but it may nevertheless lead to significant casualties once a collapse occurs. Many events have occurred in the past worldwide, e.g., the natural gas explosion that induced the Ronan Point building collapse in 1968 (UK), the terrorist attacks that induced the Murrah Federal Building collapse in 1995 and the World Trade Center collapse in 2001 (US), the improper-use-induced Rana Plaza building collapse in 2013 (Bangladesh), and the fire-induced Plasco building collapse in 2017 (Iran). Structural damage may cause a local collapse or an entire collapse, as in the above-mentioned cases. In other cases, the structures may deform to certain states, which may lead to a collapse [3,4].

In recent years, structural progressive collapse has become an important research field. Many researchers have performed numerical work (e.g., [5–11]) and experimental work (e.g., [12–20]) on the progressive collapse performances of reinforced concrete (RC) frame structures. The existing studies have focused on many aspects, including the behaviors of cast-in-place structures, precast structures, subassemblages, and whole structures; the effects of infill walls, membrane actions of slabs and arches and catenary actions of beams; Vierendeel frame actions; and the structural design method to protect against progressive collapse, etc. A recently published paper by Adam et al. [21] considered researches related to progressive collapse that had been conducted over the past twenty years to provide a very comprehensive, state-of-the-art review of this topic.

If the progressive collapse resistance capacity is insufficient, a retrofit strategy is a preferable method to mitigate the progressive collapse potential of a structure. Up until now, several studies have been conducted regarding this aspect. Crawford [22] introduced a series of retrofit methods that were suitable for mitigating the progressive collapse of multistory buildings, in which several different gravity support systems were taken into account. Hayes et al. [23] demonstrated that strengthening strategies could be used to improve the progressive collapse resistance capacity of structures. They found that the survivability of a structure could be improved by strengthening the perimeter components with seismic detailing techniques. Galal and El-Sawy [24] assessed the effectiveness of three retrofit schemes, including increasing the strength of the beams, increasing the stiffness of the beams, and increasing both the strength and stiffness of the beams. Liu [25,26] proposed a retrofit method that involved strengthening the beam-to-column connections of frame structures. Chen et al. [27] studied the behavior of frame structures when the top story was strengthened by braces. A performance-based design method for retrofitting frame structures with the adoption of braces was proposed by Tsai [28]. Kim and Shin [29] proposed a retrofit method that used prestressing tendons to strengthen frame structures. Naderi et al. [30] used a ring beam system to retrofit structures to resist progressive collapse. Adaros and Smilowitz [31] proposed a retrofit method for structures with weak perimeter moment frames and discussed the benefits and complexities of retrofitting an existing structure to meet current progressive collapse guidelines. Alrudaini [32] proposed a retrofit scheme to resist structural progressive collapse that involved including vertical steel cables parallel to the columns and a hat-braced steel frame on top of the structures to hang and support these vertical cables.

Previous studies demonstrated that the use of a fiber reinforced polymer (FRP) wrap is a cost-effective method to retrofit or upgrade structures containing deficiencies, increase gravity and lateral load capacities, and mitigate the blast effects of existing structures [33–35]. Carbon fiber reinforced polymer (CFRP) and glass fiber reinforced polymer (GFRP) wraps are the most common FRP wraps used to retrofit structures. Orton [36] conducted experimental research that showed that a CFRP wrap retrofit reduced the progressive collapse vulnerability of a frame structure. Qian and Li [37,38] conducted a series of RC flat slab tests, in which the slabs were retrofitted by externally bonded CFRP wraps to mitigate the progressive collapse potential. Feng et al. [39] and Qin et al. [40] conducted experimental and numerical research on RC beam–column substructures with different structural details and strengthening measures using GFRP wraps. Liu et al. [41] adopted CFRP strip cables to retrofit RC frame structures to resist progressive collapse.

The sustainability of a building refers to its ability to maintain its performance with an acceptable economic cost and environmental influence. Note that all of the above-mentioned studies that focused on the retrofitting of undamaged buildings had insufficient progressive collapse resistance capacity. Moreover, study on the retrofitting of damaged buildings after a progressive collapse is lacking. In many cases, the progressive collapse may only be a local behavior, e.g., flexural damages may occur at beam ends bridging the lost column but the steel rebars at the beam ends may either be only partially fractured or not at all. In these cases, as opposed to replacing the entire structure, retrofitting is an economical scheme with little environmental influence. This study aims at making a damaged structure sustainable to prevent the need for its complete reconstruction, as this would increase the economic loss and the downtime. Thus, a rapid method for retrofitting RC frames with CFRP wraps after a progressive collapse failure was proposed and verified using a progressive collapse test of a 1/3 scale, four-bay by two-story RC frame.

2. Experiment of the Frame

2.1. Test Frame Properties

A prototype frame was designed based on the Chinese building codes [42,43]. The prototype frame had a 5.1 m center-to-center distance between adjacent columns, the height of the first story was 4.2 m, and the height of the second story was 3.3 m. The test frame was a 1/3 scale, four-bay by two-story planar frame. The initial intact frame was first tested under a progressive collapse scenario in the case of the loss of the central column. Then, the damaged frame was repaired with the proposed retrofit method. Finally, the progressive collapse test was conducted again with the goal of investigating the progressive collapse behaviors of the retrofitted frame.

The design of the test frame is shown in Figure 1. The material properties of the rebars were assessed based on tensile strength tests. Standard concrete prisms of 150 mm × 150 mm × 300 mm were used for concrete compressive tests. The measured compressive strengths were 41.3 MPa and 31.8 Mpa for the first and second story concretes, respectively. More information on this test frame was provided in detail in previous studies [11,18,19]. A high-strength concrete grouting material (CGM) and CFRP wrap were used in the retrofit procedure. The CGM was made of cement, sand, early-strength additive, etc. The compressive strength of the CGM was 60.0 Mpa and could be reached within one day. Thus, it was possible to conduct a very rapid retrofit procedure. To determine the material properties of the CFRP wrap, six flat coupons with a width of 25 mm and length of 200 mm were tested to fracture. Three of these coupons contained one wrap layer, whereas the other three coupons contained two layers. The tested ultimate strength of the CFRP wrap was 4340 Mpa, and the elastic modulus was 240,000 Mpa. The tested thickness of the CFRP wrap was 0.167 mm. The material properties of the rebars, concrete, grouting, and CFRP wrap are given in Table 1.

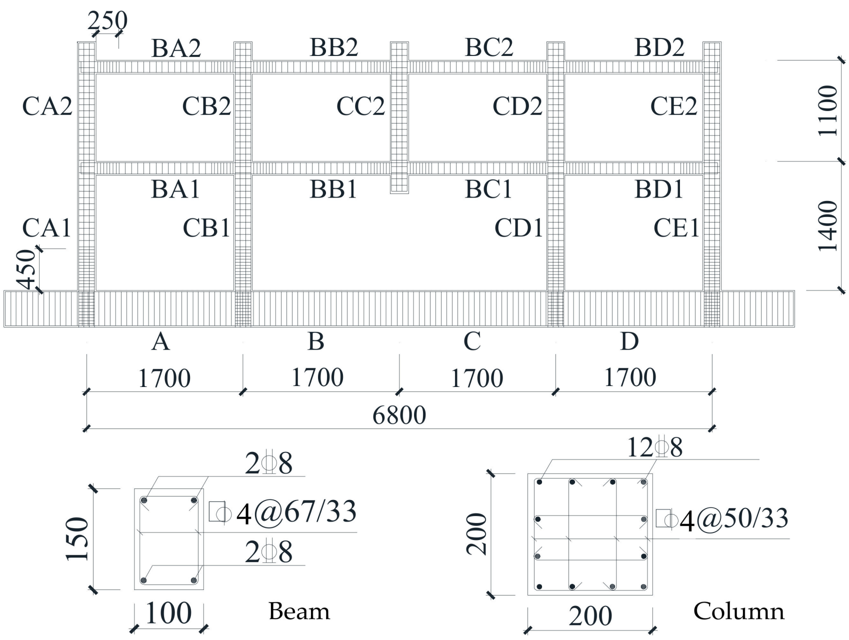

Figure 1. Design details of test frame (unit: mm), where A. ⌽ denotes the diameter of the deformed horizontal rebar and ⌽ denotes the diameter of the plain stirrup rebar.

Table 1. Material properties of the test frame.

Material	Item	Property
Concrete	Compressive Strength	First Story: 41 MPa Second Story: 32 MPa
8 mm diameter rebar	Yield strength Ultimate strength Strain at fracture	415 MPa 588 MPa 0.18
4 mm diameter stirrup	Yield strength Ultimate strength Strain at fracture	235 MPa 322 MPa 0.31
Concrete grouting CFRP wrap (thickness: 0.167 mm)	Compressive strength Ultimate strength Strain at fracture	60 MPa 4340 MPa 0.0178

2.2. Test Setup and Procedure

The progressive collapse scenario was simulated by applying a quasistatic vertical load on the center column of the frame as shown in Figure 2. A hydraulic jack, placed at the top of the center column, was used to apply a constant vertical load. A hand jack, placed below the center column, was unloaded step by step with displacement control. Because the loading procedure was slow, the strain ratio effect was not considered. In order to prevent any undesired out-of-plane movement of the frame, two horizontal collar devices installed on the lateral braces (each collar device consisted of a pair of rollers in opposite directions out of the frame plane) were attached to two sides of the center column so that the center column could only move vertically. Similarly, four vertical collar devices were attached to both sides of the adjacent and external columns. There were 5 mm gaps provided between the rollers and the column surfaces to avoid unwanted frictional forces on the columns in the initial loading stage.

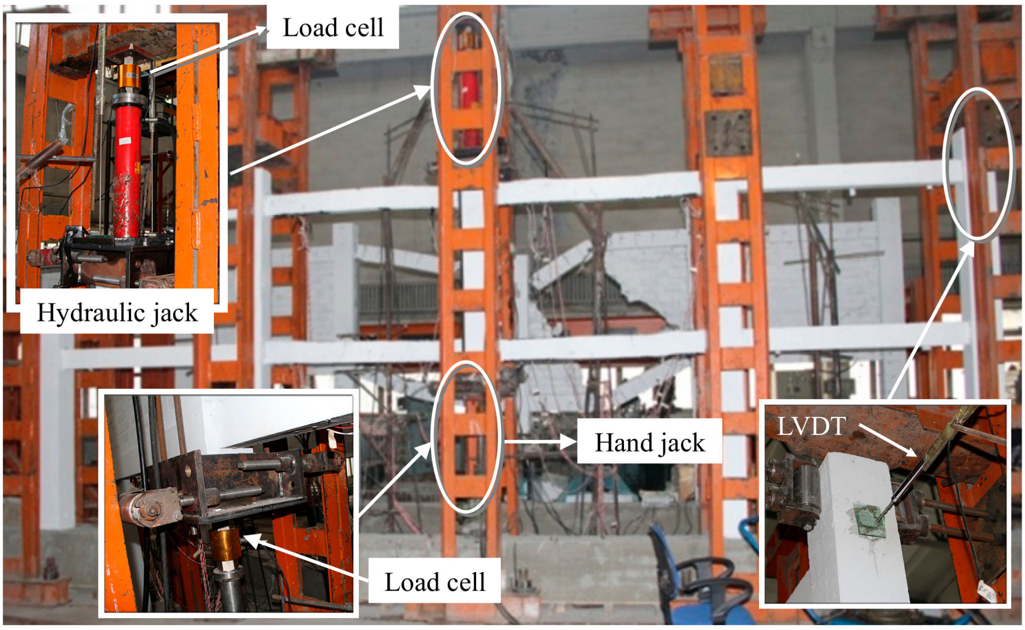

Figure 2. Loading and measurement systems.

As shown in Figure 3, two load cells above and below the center column were used to measure the applied vertical load, i.e., the progressive collapse resistance force that came from the center column. Two vertical linear variable differential transformers (LVDTs) and two relative displacement meters were placed above the center column to measure its vertical displacement. Eight horizontal LVDTs were placed at each beam–column joint in order to measure the horizontal displacements of the adjacent and external columns. Figure 4 shows the experimental procedure of the progressive collapse tests performed on the initial frame and retrofitted frame.

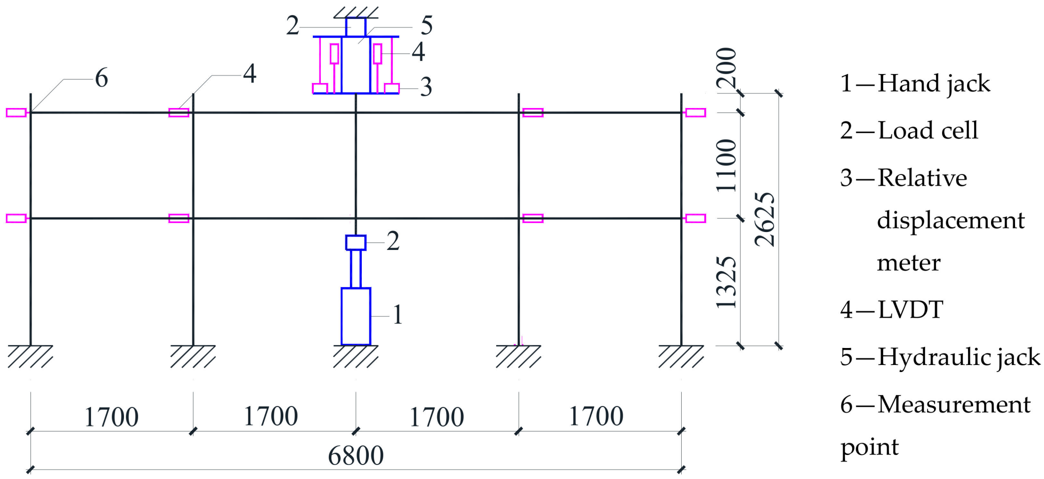

Figure 3. Test instrumentation (unit: mm).

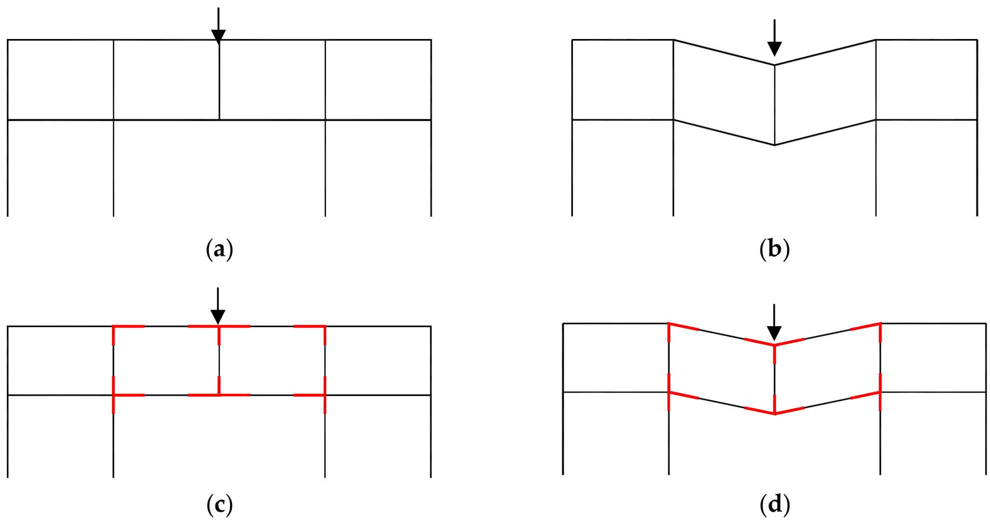

Figure 4. Procedure of progressive collapse tests performed on initial and retrofitted frames: (**a**) Initial frame; (**b**) First test; (**c**) Retrofitted frame; (**d**) Second test.

2.3. Test Results of the Initial Frame

Figure 5 shows the resistance force versus vertical displacement of the center column for the initial frame. Some test results of the initial frame had been provided in previous studies [11,18,19], in which the frame underwent three loading stages: the initial stage (OA), compressive stage (AC), and catenary stage (CD). Point B corresponded to the vertical displacement of the center column at the maximum resistance force before the compressive stage, and the rebars fractured at points D and E. The final failure mode of the frame at the end of the test is shown in Figure 6, at the vertical displacement of 418 mm. It is observed that the damages were mainly concentrated at the beam ends in bays B and C (see Figure 6a–h). Some cracks developed in the concrete surface in the first-story columns in bays B and C, but the damage was slight (see Figure 6i, j). The damage to the beams in bays A and D and the other columns was also slight. The rebars in the top left end of beam BB2 fractured at vertical displacements of 317 mm and 346 mm, leading to two sharp drops in the resistance force, as shown in Figure 5. At a vertical displacement of 354 mm, both of the rebars in the top right end of beam BC2 fractured. The rebars in the bottom left end of beam BC1 fractured at vertical displacements of 354 mm and 359 mm.

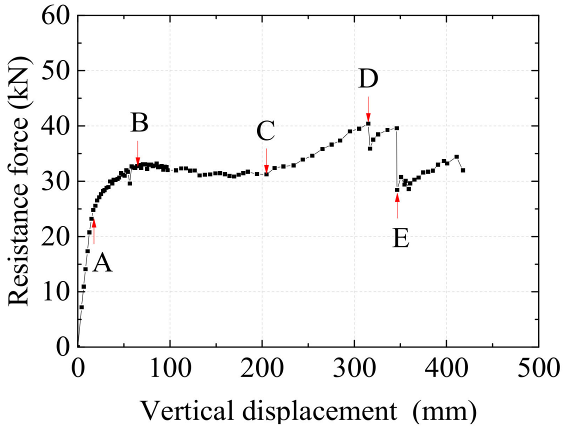

Figure 5. Resistance force versus vertical displacement of the central column for the initial frame.

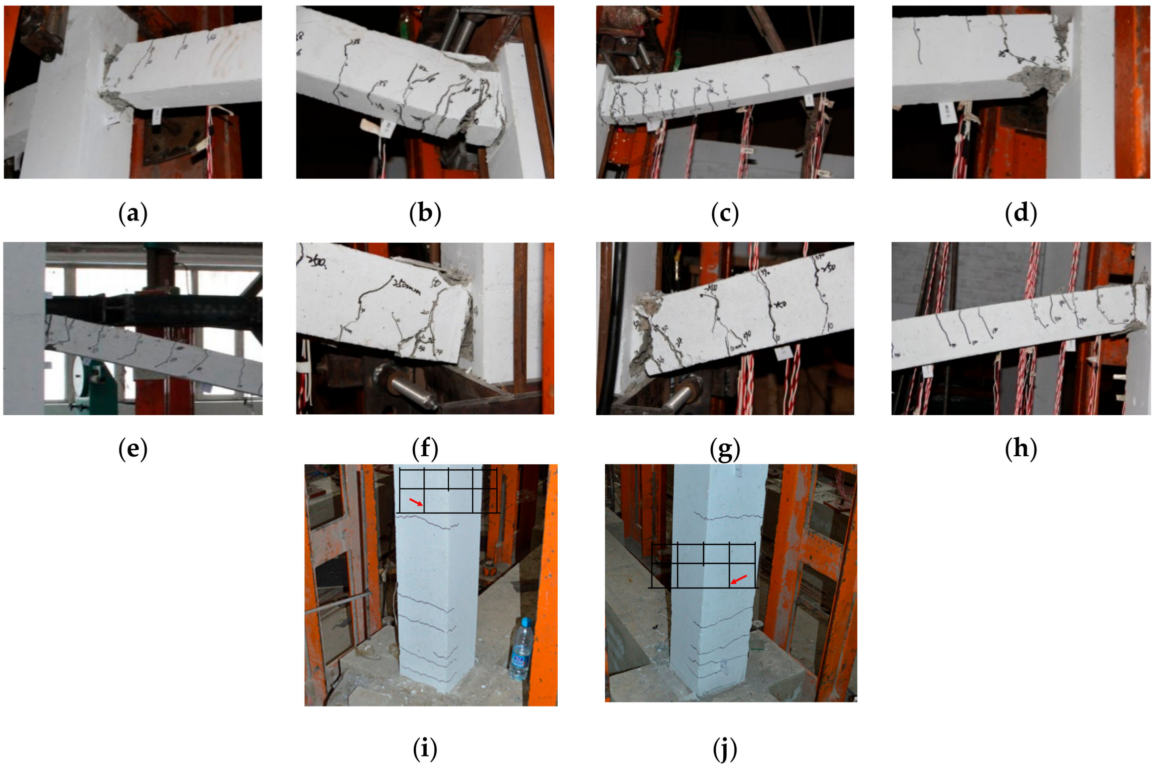

Figure 6. Cracks of the initial frame at end of test: (**a**) BB2 left; (**b**) BB2 right; (**c**) BC2 left; (**d**) BC2 right; (**e**) BB1 left; (**f**) BB1 right; (**g**) BC1 left; (**h**) BC1 right; (**i**) CB1 bottom; (**j**) CD1 bottom.

2.4. Retrofit of the Test Frame

Based on observations from the progressive collapse test results of the initial frame, only repairs on the beams were needed in the retrofit process. The retrofit of the frame was conducted according to the following procedure.

(1) After the first test, the frame was damaged and deformed to a specific vertical displacement (Figure 7a). Push the frame upward from the progressive collapse state to return to the undeformed state (Figure 7b).
(2) Remove the damaged concrete near the beam–column joints in bays B and C (damaged bay) and straighten the rebars if their diameters did not show obvious shrinkage (Figure 7c). In this test, the extent of the removed concrete was 250 mm from the column surfaces. This range was determined because it was slightly larger than the plastic hinge length (set as one beam height of 150 mm in this case) plus the required weld length between the new and original rebars (smaller than 100 mm in this case). The stirrups within this range were also removed. After removing the damaged concrete and stirrups, the beam segment in the center region of the beams could deform downward due to the gravity action of the beam segment. At this moment, the resistance force of the frame in the damaged bay was only provided by the dowel action of the rebars. Therefore, if necessary, braces could be installed below the beam segment in the center region of the beam to prevent the potential downward movement of the beam segment (Figure 7d).
(3) Replace the rebars that were fractured and those whose diameters showed obvious shrinkage within the range of the removed concrete (Figure 7e). These replacements were implemented using new rebars instead of the fractured or shrunken segments of the original rebars. In this test, the length of the new rebar was 450 mm, with one end planted in the column with a length of 200 mm (larger than the required anchor length) and the other end welded to the original rebar with a weld length of 100 mm. The original rebars, which needed to be replaced, were cut within a range of 0–150 mm from the column surface. Because uncertainty existed in the performance degradation of the unreplaced rebars, the new rebars had a diameter of 10 mm, which was slightly larger than that of the original rebars (8 mm).
(4) The molding board was built within the range of the removed concrete (Figure 7f) and high-strength CGM was poured into it. The molding board was removed after one day, when the strength of the CGM had developed. In order to use the CFRP wrap, the four edges of the beam cross-section in the damaged bays were ground to obtain rounded edges in the area where the wrap was used. In this test, the edge was ground up to 500 mm from the column surface, which was two times the length of the removed concrete.
(5) Bond the CFRP wraps as shown in Figure 7g. Figure 8 shows the detailed dimensions of the bonded CFRP wraps and their positions. To provide a flexural-resistance capacity, two layers were bonded at the top and bottom surfaces of the beams along the beam's axial direction and extended to column surfaces. Thereafter, to provide an anchor action and a shear-resistance capacity, two layers that encircled the beams and columns were bonded.

The adhesive for the CFRP wraps reached its maximum strength in approximately two days. The total period of the retrofit process, i.e., from the start to recovering its original capacity, was only approximately three days. After the retrofit, a progressive collapse test was conducted again (Figure 7h). It is worth noting that the damaged column should also be repaired in practical retrofit situations. However, the damaged column was not repaired in this study because the goal was to conduct the progressive collapse test again.

(**a**) (**b**) (**c**) (**d**) (**e**) (**f**) (**g**) (**h**)

Figure 7. Retrofit procedure of the frame: (**a**) Frame after progressive collapse; (**b**) Restore to undeformed status; (**c**) Remove damaged concrete and straighten rebars; (**d**) Brace frame to keep its undeformed status; € Replace damaged rebars; (**f**) Build molding board and pour high strength CGM; (**g**) Remove molding board and bond CFRP wrap; (**h**) Retest on retrofitted frame.

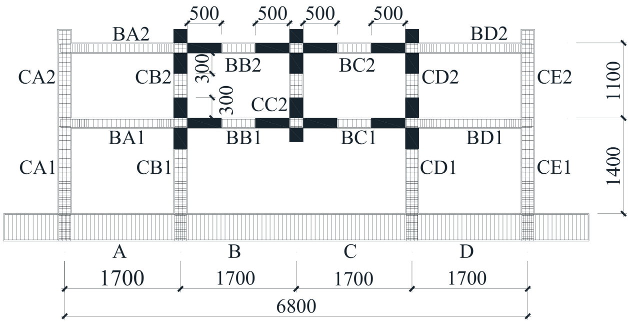

Figure 8. Retrofit of frame using CFRP wrap (Unit: mm).

2.5. Test Results of the Retrofitted Frame

The resistance force versus vertical displacement of the center column of the retrofitted frame is compared with that of the initial frame in Figure 9. It is observed that the retrofitted frame provided a larger resistance force than the initial frame. There was no catenary stage until the CFRP wrap fractured. The fractures of the CFRP wraps led to several large sharp drops in the resistance force curve, as shown in Figure 9. The first obvious drop at the vertical displacement of 231 mm was due to the CFRP wrap fracture. Thereafter, several drops occurred due to sequential fractures of the CFRP wrap and rebar at additional positions. Figure 10 shows a comparison between the horizontal displacements of the beam–column joints at the adjacent and external columns versus the vertical displacement of the center column for the retrofitted and initial frames. It is observed that the adjacent and external beam–column joints first moved outward and reached their maximum horizontal displacement values. Thereafter, as the vertical displacement increased, the beam–column joints moved back and inward until the end of the test. Generally, catenary actions in the beams in damaged bays occurred when beam–column joints moved back and started to have inward displacement when compared to that at their initial positions (at a horizontal displacement of 0 mm). As shown in Figure 10, the catenary stage of the retrofitted frame occurred later than that of the initial frame. For the retrofitted and initial frames, Figures 9 and 10 show that the initial secant stiffnesses were 1.67 kN/mm and 1.57 kN/mm, and the maximum resistance forces in the compressive stage were 50.7 kN and 33.2 kN, respectively. The initial secant stiffness and maximum resistance force of the retrofitted frame were 6.37% and 52.71% larger than those of the initial frame, respectively. Figure 11 shows the progressive collapse process of the retrofitted frame corresponding to different vertical displacements of the center column. The failure modes of the initial and retrofitted frames at the end of the tests are compared in Figure 12. The damage to the initial frame was concentrated at the beam ends, whereas that of the retrofitted frame was concentrated at the beam ends and the regions around the edges of the CFRP wraps. Figure 13 shows the cracks of the retrofitted frame at the end of the test. Compared with Figure 6, the cracks in the retrofitted frame were concentrated at the beam–column interfaces because the CFRP wraps prevented the cracks from propagating to the beam end regions.

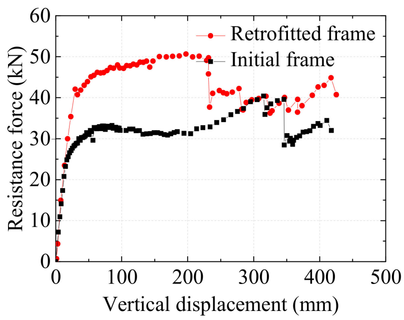

Figure 9. Comparison of resistance force versus vertical displacement of central column for retrofitted and initial frames.

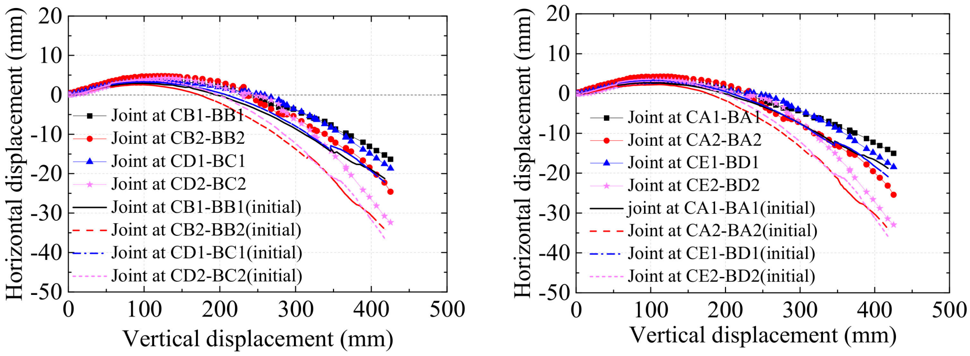

(**a**) (**b**)

Figure 10. Comparison of horizontal displacement of joints versus vertical displacement of center column for retrofitted and initial frames: (**a**) Adjacent columns; (**b**) External columns.

(**a**) (**b**)

(**c**) (**d**)

(**e**) (**f**)

Figure 11. *Cont.*

(**g**) (**h**)

Figure 11. Progressive collapse process of retrofitted frame: (**a**) Vertical displacement at 30 mm (frame); (**b**) Vertical displacement at 30 mm (joint); (**c**) Vertical displacement at 130 mm (frame); (**d**) Vertical displacement at 130 mm (joint); € Vertical displacement at 230 mm (frame); (**f**) Vertical displacement at 230 mm (joint); (**g**) Vertical displacement at 420 mm (frame); (**h**) Vertical displacement at 420 mm (joint).

(**a**) (**b**)

Figure 12. Comparison of failure modes of retrofitted and initial frames at end of tests: (**a**) First test [18]; (**b**) Second test.

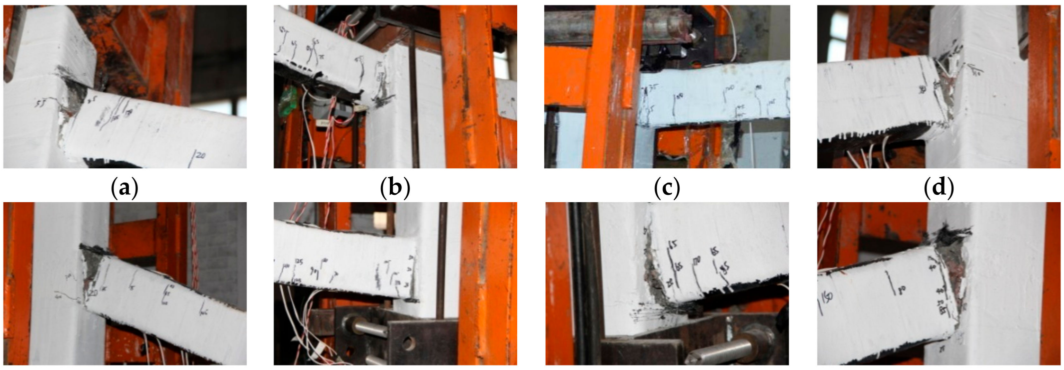

(**a**) (**b**) (**c**) (**d**)

(**e**) (**f**) (**g**) (**h**)

Figure 13. Cracks of the retrofitted frame at end of test: (**a**) BB2 left; (**b**) BB2 right; (**c**) BC2 left; (**d**) BC2 right; € BB1 left; (**f**) BB1 right; (**g**) BC1 left; (**h**) BC1 right.

3. Numerical Analysis on the Retrofitted Frame

3.1. Finite Element Model

To simulate the behaviors of the retrofitted and initial frames, finite element models were developed using the OpenSees software [44]. A detailed explanation of the generation and analyses of these finite element models, including the elements, meshes, and material models, is provided in the following sections. It should be mentioned that the potential degradation of the mechanical performance of unfractured rebars was not considered in the simulations.

Figure 14a shows the finite element modeling strategy for the CFRP-retrofitted frame, in which the positions marked with red solid lines are bonded with the CFRP wraps. The subframe shown in Figure 14b illustrates the finite element meshes of the model. Eight elements were used for each frame member. The same type of beam–column elements were used at the positions marked with the same number. The element type in positions with the number "1" was an elastic beam element (elasticBeamColumn in OpenSees), which was assigned a very large material stiffness in order to simulate the effect of a rigid region due to the beam–column joint. The element type at all of the other positions was the force-based beam–column element (forceBeamColumn in OpenSees). Two Gauss–Lobatto integration points were used for each element to prevent numerical instability and maintain the accuracy of this type of element. A corotational coordinate transformation was used to take into account the geometrical nonlinearity. The member cross-sections were modeled using fiber-section models. Figure 14c–f illustrates the modeling of the member cross-sections in positions numbered "2", "4", "5", and "6" in Figure 14b. The modeling of the member cross-section in a position with the number "3" was similar to that for position "2", but the effect from stirrups was also considered when the confinement effect on the concrete was calculated. The member cross-sections in positions with the number "3" had two confinement effects on the concrete (i.e., CFRP and stirrup). In the fiber-section models, the CFRP wraps bonded at the top and bottom surfaces of the beam were considered as fibers in the modeling, while the CFRP wraps bonded at the side surfaces of the beam were considered as confinement effects on the concrete similar to the confinement effects of stirrups.

The material behaviors for the confined (by stirrups) and unconfined concrete were assumed to follow the Kent–Scott–Park constitutive model (Concrete01 in OpenSees) [45]. The material behaviors for the confined (by CFRP, and CFRP as well as stirrups) concrete were also assumed to follow the Kent–Scott–Park constitutive model, but the control parameters in the stress–strain envelope curve were calculated using the method proposed by Wang et al. [46] for CFRP-confined concrete. The rebar materials were modeled using a bilinear material model (Steel01 in OpenSees) with an elastic modulus of 2.0×10^5 Mpa. The CFRP wrap material was modeled using an elastic-perfectly plastic material model (ElasticPP in OpenSees) with zero compression capacity. The MinMax material model was used to mimic fractures of the rebars and CFRP wraps. The material parameters used in the constitutive models were determined based on the test results, as listed in Table 1.

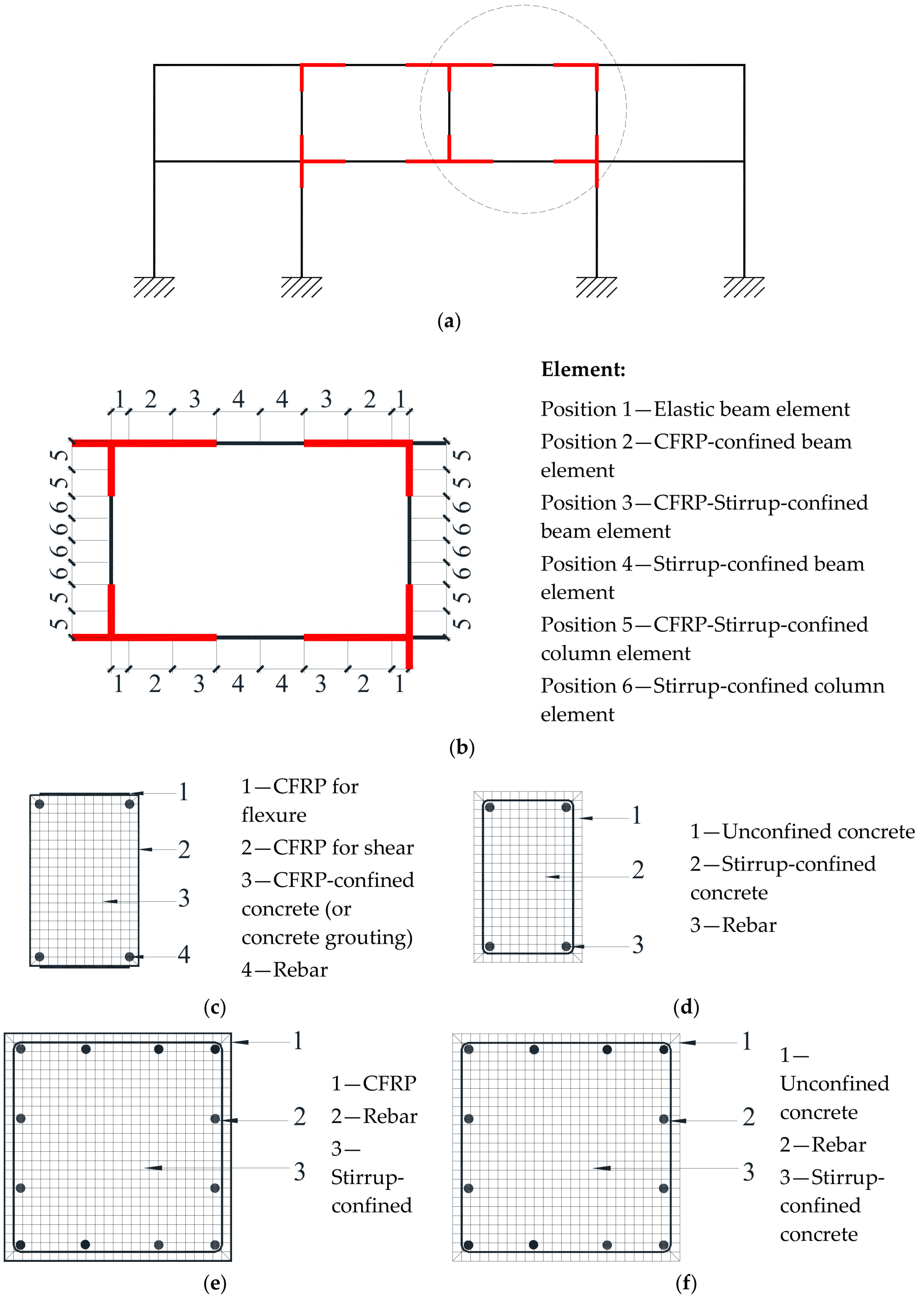

Figure 14. Finite element modeling strategy for the CFRP-retrofitted frame: (**a**) Finite element model of retrofitted frame; (**b**) Beam and column element meshes; (**c**) Beam element—Position 2; (**d**) Beam element—Position 4; € Column element—Position 5; (**f**) Column element—Position 6.

3.2. Verification of the Numerical Analysis

During the numerical simulation, the center column was pushed down using displacement control to mimic the loading strategy used in the test. Figure 15 shows the deformation of the frame in the numerical analyses. The values of the resistance force versus vertical displacement of the center column of the frame obtained in the numerical simulation and test are compared in Figure 16. Figure 17 shows the numerical simulation and test results for the horizontal displacements of the beam–column joints at the adjacent and external columns versus the vertical displacement of the center column after the retrofit. In these figures, it can be observed that the proposed numerical model provided a good prediction of the experimental responses.

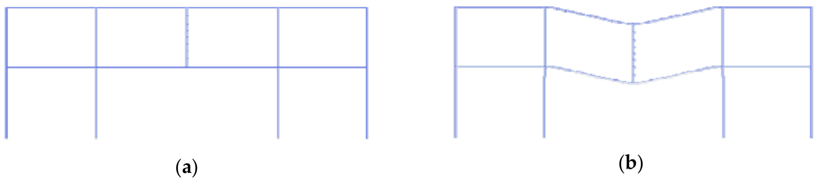

Figure 15. Deformations in numerical analyses: (**a**) Before loading; (**b**) After loading.

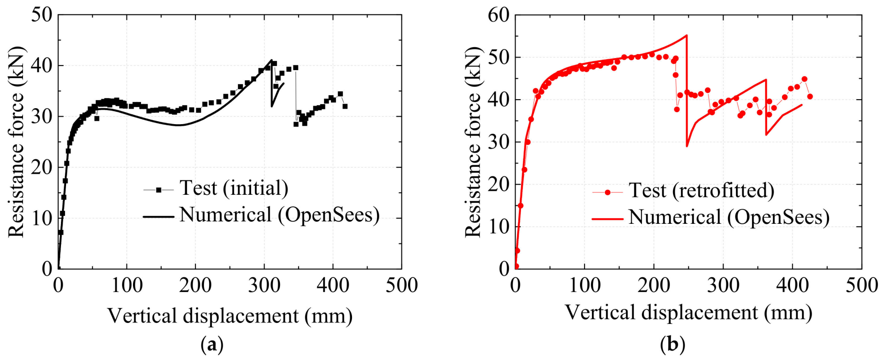

Figure 16. Numerical simulation and test resistance force values versus vertical displacement of center column for frames: (**a**) First test (initial frame); (**b**) Second test (retrofitted frame).

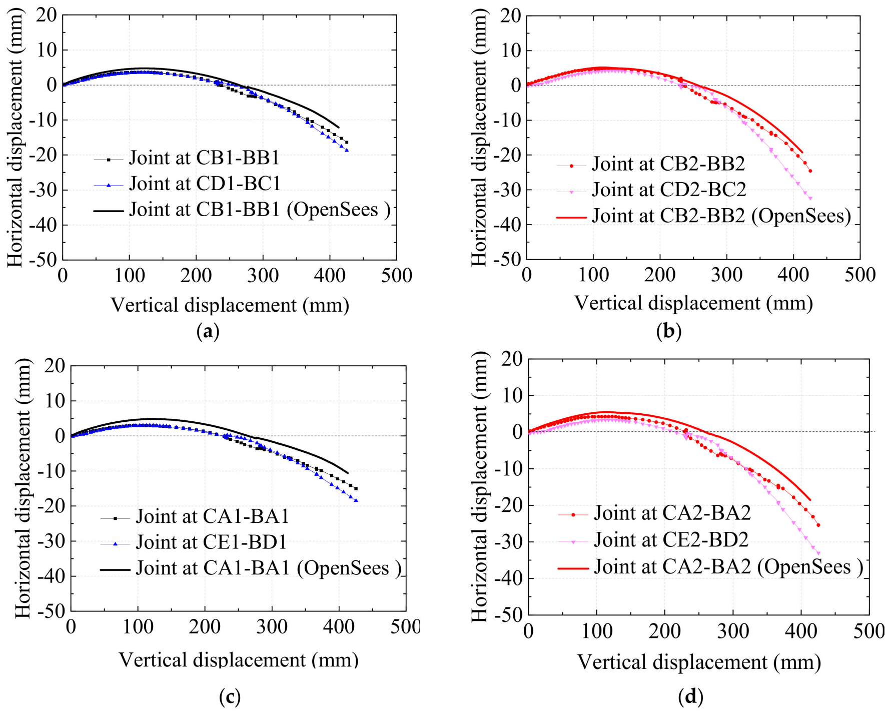

Figure 17. Numerical simulation and test values for horizontal displacements of joints versus vertical displacement of center column for retrofitted frame: (**a**) Adjacent columns (first story); (**b**) Adjacent columns (second story); (**c**) External columns (first story); (**d**) External columns (second story).

4. Retrofit Design Method and Design Example

4.1. Design Method

It should be mentioned that the retrofit procedure presented in Section 2.4 is a scheme of implementation rather than a retrofit design procedure. This section proposes a design method for retrofitting an RC frame after a progressive collapse. The retrofit design method aims to guarantee that the beam (or column) ends have sufficient moment resistances, shear resistances, and "strong-column and weak-beam" failure mechanisms. After the retrofit, the progressive collapse resistance capacity of the retrofitted frame should be no less than that of the initial frame.

4.1.1. Moment Resistance of Cross-Section

Based on the equilibrium of the forces in a member cross-section, the moment resistances of cross-sections at the beam ends for the CFRP-retrofitted frame and initial frame can be calculated using Equations (1) to (4) [43,47]. After the retrofit, the moment resistance calculated by Equation (1) is expected to be larger than that found using Equation (3).

$$M = \alpha_1 f_c bx(h - \frac{x}{2}) + f'_y A'_s(h - a') - f_y A_s(h - h_0) \tag{1}$$

$$\alpha_1 f_c bx = f_y A_s + f_f A_{fe} - f'_y A'_s \tag{2}$$

$$M = \alpha_1 f_c bx(h_0 - \frac{x}{2}) + f'_y A'_s(h_0 - a') \tag{3}$$

$$\alpha_1 f_c bx = f_y A_s - f'_y A'_s \tag{4}$$

where M is the moment resistance of the cross-section; x is the height of the concrete compression zone, which should satisfy $x \geq 2a'$, where a' is the closet distance from the resultant force point of the compression rebars to the cross-section edge; b and h are the width and height of the cross-section, respectively; h_0 is the farthest distance from the resultant force point of the tension rebars to the cross-section edge; α_1 is a coefficient used to consider the stress shape of the concrete compression zone, which is commonly set at 1.0 for concrete with a compression strength lower than 50 MPa and at 0.94 for concrete with a compression strength of 80 Mpa (with linear interpolation between 50 and 80 Mpa); f_c, f_y, f'_y, f_f, A_s, A'_s, and A_{fe} are the concrete compression strength, yield strength of the tension rebars, yield strength of the compression rebars, tension strength of the CRFP wraps, area of the tension rebars, area of the compression rebars, and area of the CFRP wraps, respectively.

4.1.2. Shear Resistance of Cross-Section

As reported in Section 2.4, the stirrups at the beam ends were removed, and their functions were replaced by the CFRP wraps. The shear resistance values of the cross-sections at the beam ends of the CFRP-retrofitted frame and initial frame can be calculated using Equations (5) and (6), respectively [43,47]. After the retrofit, the shear resistance calculated by Equation (5) was expected to be larger than that found using Equation (6).

$$V = \alpha_{cv} f_t bh_0 + \psi_{vb} f_f \frac{A_f}{s_f} h_f \tag{5}$$

$$V = \alpha_{cv} f_t bh_0 + f_{yv} \cdot \frac{A_{sv}}{s} \cdot h_0 \tag{6}$$

where V is the shear resistance of the cross-section; α_{cv} is a coefficient that is generally set at 0.7; f_t is the tension strength of the concrete, which is assumed to be $0.1 f_c$; ψ_{vb} is a coefficient that considers the shear strength reduction due to anchoring, which was assumed to be 0.5 in this study; f_f is the tension strength of the CRFP wraps, where a value of $0.28 f_f$ is adopted instead of f_f when it is used in a shear resistant retrofit according to the design codes; A_f/s_f is the mean cross-sectional area of the

CFRP wraps within length s_f; h_f is the height of the CFRP wraps on the lateral side of the beam; f_{yv} is the strength of the stirrups; A_{sv}/s is the mean cross-sectional area of the stirrups within length s; h_0 is the farthest distance from the resultant force point of the tension rebars to the cross-section edge.

4.1.3. Other Considerations in Design

The "strong-column and weak-beam" mechanism (if the frame is a seismic structure) and minimum dimension requirement of the beam cross-section to resist a shear force should also be taken into account in the design method. Unlike the calculation of the moment resistance of the beam cross-section by Equations (1) to (4), the calculation of the moment resistance of the column cross-section is relevant to the axial force in the column [43,47]. However, the axial force is not easy to calculate in some cases. In order to avoid the calculation of the axial force in the column and facilitate the retrofit design procedure, it is advised that the retrofit be conducted at both beam ends and column ends (as shown in Figure 8). The CFRP wraps bonded on a column can have a length equal to the width of the column cross-section (commonly equal to the plastic hinge length). Because the initial frame is designed to satisfy the "strong-column and weak-beam" mechanism, in this way, the "strong-column and weak-beam" mechanism can be commonly maintained without further verification. Meanwhile, the CFRP wraps bonded on the column can be used for anchoring the CFRP wraps that are bonded to the beams. The minimum dimension requirement of the beam cross-section to resist the shear force is relevant to the concrete compression strength and cross-sectional area [43,47]. Because the strength of the CGM adopted in the retrofit was larger than or similar to that of the initially used concrete, and the cross-sectional area remained unchanged during the retrofit, the minimum dimension requirement of the beam cross-section to resist the shear force was automatically satisfied. In order to avoid any potential fragile damage to the CFRP wraps, at least two layers were used.

4.2. Verification of the Test Frame

In Section 2.5, Figure 9 showed that the retrofit provided conservative results compared to the initial frame. This section discusses an improved design for the test frame to illustrate the design method developed in Section 4.1. After the redesign, the changes compared to the frame presented in Section 2.4 included the following: (1) the compression strengths of the CGMs used for the first and second stories were 30 Mpa and 40 Mpa, respectively, and rebars with diameters of 8 mm were used to replace the fractured rebars and those with diameters that had obviously shrunk within the areas of the removed concrete; (2) the length of the CFRP wraps bonded on the column was 200 mm. Table 2 compares the calculated cross-section moment resistance and shear resistance at the beam ends. It shows that the design results satisfied the retrofit target. The moment resistances of the beam ends obtained from the improved retrofit were closer to those of the initial frame. The shear resistances of the beam ends were the same between the retrofit and the improved retrofit. It is worth noting that the shear resistance of the improved retrofit listed in Table 2 is still very conservative and could be further optimized in practical situations using several discrete CFRP wrap strips rather than one continuous strip, although the use of one continuous strip, as in this study, is the most convenient in some cases. Figure 18 shows that the improved retrofit design also provides a conservative resistance force but with a more economical cost. A similar retrofit method is applied in the progressive collapse case with external column damage, such as shown in Figure 19a–d. Figure 19e shows that the retrofit provides satisfactory results for restoring the structural performance, which reaches the goal of recovering the original structural strength.

Table 2. Improved retrofit design for the test frame.

	Calculation Method	Position	Result: Initial	Result: Retrofit	Result: Improved Retrofit	Ratios to Initial	Satisfy
Moment resistance	After retrofit: Equation (1a) Initial: Equation (2a)	Beam end at first story	22.12 kN·m	27.02 kN·m	23.79 kN·m	1.22, 1.08	Yes
		Beam end at second story	18.29 kN·m	27.02 kN·m	22.91 kN·m	1.48, 1.25	Yes
Shear resistance	After retrofit: Equation (3) Initial: Equation (4)	Beam end at first story	61.04 kN	115.48 kN	115.48 kN	1.89, 1.89	Yes
		Beam end at second story	52.79 kN	115.48 kN	115.48 kN	2.19, 2.19	Yes

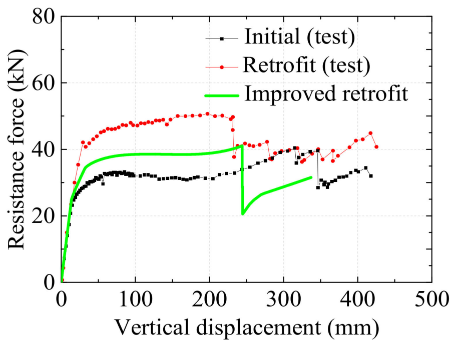

Figure 18. Resistance force versus vertical displacement of center column for test frame with improved retrofit design.

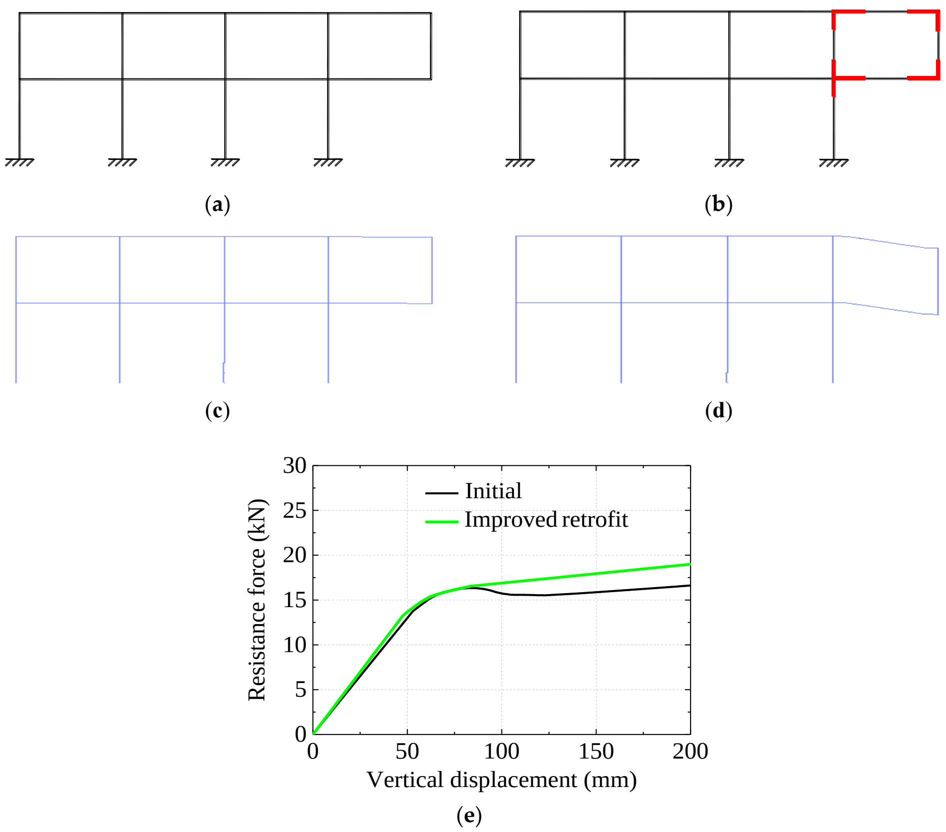

Figure 19. Resistance force versus vertical displacement of external column for test frame with improved retrofit design; (**a**) Loss of external column; (**b**) Retrofit positions; (**c**) Deformation in numerical analyses: Before loading; (**d**) Deformation in numerical analyses: After loading; (**e**) Resistance force versus vertical displacement.

5. Economic Cost and Environmental Impact

In addition to the previously discussed structural performance analyses, the sustainability requires a comparison of the economic cost and environmental impact. The test frame was only a planar specimen and was not suitable for quantifiably demonstrating the economic cost of a retrofit. An RC frame (six-story, five-bay by three-bay) designed according to the Chinese building codes [42,43] was analyzed [48] using the FEMA P-58 PACT software [49]. The results showed that the reconstruction cost (including the demolition) for the six-story RC frame was approximately 0.77 million dollars and this cost did not consider the indirect loss resulting from the downtime, which would be more than 600 workdays. Therefore, if the proposed rapid retrofit method could be used, the economic benefit would be obvious. In relation to the environmental impact, a rapid retrofit and local repair would significantly reduce the adverse influences on the environment.

6. Conclusions and Discussion

This study focused on a method to increase the sustainability of a structure after a progressive collapse. In many cases, a local collapse, rather than the entire collapse of a structure, may occur during progressive collapse scenarios, with only the beam ends deformed to a certain deformation level, leaving the structure in a repairable state. The retrofitting of structures subjected to this type of progressive collapse was studied. The conclusions are as follows:

(1) A progressive collapse test on a CFRP-retrofitted 1/3 scale, four-bay by two-story RC frame was conducted. The progressive collapse resistance forces, crack developments, and local and global failure modes of the CFRP-retrofitted RC frame were presented. The test showed that the retrofit process could be completed within three days, which revealed that the structure had very good resilience, allowing it to rapidly recover its functions. A numerical analysis was also performed to verify the test results.

(2) A retrofit design method was proposed that uses CFRP wraps for structures after a progressive collapse. The test retrofitted RC frame was redesigned using the proposed retrofit design method, which showed that a more economical retrofit scheme could be achieved using the design method. The CFRP-retrofit method could be a preferable and economical method to handle structures that have suffered a progressive collapse.

(3) Retrofitting a structure subjected to a progressive collapse instead of reconstructing the whole structure is a more rational choice and gives the structure a chance for sustainable use in the future. In addition to recovering the performance with an acceptable economic cost, a retrofit would obviously reduce the downtime-induced economic loss and environmental impact from a long period of construction (demolition and reconstruction).

(4) The retrofit could be quick and easy for the tested planar frame. For real RC frames suffering a column loss, the adjacent RC slabs would also be deformed. This study ignored the presence of slabs, which in practice will affect the retrofitting process. For example, if concrete slabs are present ("T-shaped" or "L-shaped" beams in that case), it will not be easy to wrap an entire damaged beam with CFRP. However, this issue can easily be resolved because it would still be possible to use the retrofit strategy proposed in this study, with only minor changes made to retrofit the "T-shaped" or "L-shaped" beams in relation to the moment and shear resistances of the member cross-sections.

Author Contributions: Conceptualization, S.L.; methodology, S.L. and S.S.; validation, S.S. and H.Z.; formal analysis, S.L., S.S., and Y.L.; writing, S.L. and Y.L.; funding acquisition, S.L.

Funding: This research was supported by the National Natural Science Foundation of China (Grant No. 51578202, 41861134010), Natural Science Foundation of Heilongjiang (YQ2019E021), and Postdoctoral Scientific Research Development Fund (LBH-Q16099). The financial supports of these research funds are greatly appreciated by the authors.

Acknowledgments: The CFRP wrap was provided by Zhenyu Wang at Harbin Institute of Technology, who is greatly appreciated.

Conflicts of Interest: The authors declare no conflict of interest.

References

1. ASCE/SEI 7-10. *Seismic Evaluation and Retrofit of Existing Buildings*; American Society of Civil Engineers: Reston, VA, USA, 2010.
2. UFC4-023-03. *Unified Facilities Criteria: Design of Buildings to Resist Progressive Collapse*; Department of Defense: Washington, DC, USA, 2016.
3. Sasani, M.; Sagiroglu, S. Progressive collapse resistance of Hotel San Diego. *J. Struct. Eng.* **2008**, *134*, 76–83. [CrossRef]
4. Song, B.I.; Giriunas, K.A.; Sezen, H. Progressive collapse testing and analysis of a steel frame building. *J. Constr. Steel Res.* **2014**, *94*, 76–83. [CrossRef]
5. Elkoly, S.; El-Ariss, B. Progressive collapse evaluation of externally mitigated reinforced concrete beams. *Eng. Fail. Anal.* **2014**, *40*, 33–47. [CrossRef]
6. Amiri, S.; Saffari, H.; Mashhadi, J. Assessment of dynamic increase factor for progressive collapse analysis of RC structures. *Eng. Fail. Anal.* **2018**, *84*, 300–310. [CrossRef]
7. Bredean, L.A.; Botez, M.D. The influence of beams design and the slabs effect on the progressive collapse resisting mechanisms development for RC framed structures. *Eng. Fail. Anal.* **2018**, *91*, 527–542. [CrossRef]
8. Yu, J.; Luo, L.Z.; Li, Y. Numerical study of progressive collapse resistance of RC beam-slab substructures under perimeter column removal scenarios. *Eng. Struct.* **2018**, *159*, 14–27. [CrossRef]
9. Kunnath, S.K.; Bao, Y.H.; El-Tawil, S. Advances in computational simulation of gravity-induced disproportionate collapse of RC frame buildings. *J. Struct. Eng.* **2018**, *144*, 03117003-1-18. [CrossRef]
10. Feng, D.C.; Xie, S.C.; Deng, W.N.; Ding, Z.D. Probabilistic failure analysis of reinforced concrete beam-column sub-assemblage under column removal scenario. *Eng. Fail. Anal.* **2019**, *100*, 381–392. [CrossRef]
11. Li, S.; Kose, M.M.; Shan, S.D.; Sezen, H. Modeling methods for collapse analysis of reinforced concrete frames with infill walls. *J. Struct. Eng.* **2019**, *145*, 04019011-1-12. [CrossRef]
12. Yi, W.J.; He, Q.F.; Xiao, Y.; Kunnath, S.K. Experimental study on progressive collapse-resistant behavior of reinforced concrete frame structures. *Aci Struct. J.* **2008**, *105*, 433–439. [CrossRef]
13. Sasani, M.; Sagiroglu, S. Progressive collapse resistance of Hotel San Diego. *J. Struct. Eng.* **2008**, *134*, 478–488. [CrossRef]
14. Yu, J.; Tan, K.H. Experimental and numerical investigation on progressive collapse resistance of reinforced concrete beam column sub-assemblages. *Eng. Struct.* **2013**, *55*, 90–106. [CrossRef]
15. Pham, X.D.; Tan, K.H. Experimental study of beam-slab substructures subjected to a penultimate-internal column loss. *Eng. Struct.* **2013**, *55*, 2–15. [CrossRef]
16. Stinger, S.M.; Orton, S.L. Experimental evaluation of disproportionate collapse resistance in reinforced concrete frames. *Aci Struct. J* **2013**, *110*, 521–530.
17. Keyvani, L.; Sasani, M.; Mirzaei, Y. Compressive membrane action in progressive collapse resistance of RC flat plates. *Eng. Struct.* **2014**, *59*, 554–564. [CrossRef]
18. Shan, S.D.; Li, S.; Xu, S.Y.; Xie, L.L. Experimental study on the progressive collapse performance of RC frames with infill walls. *Eng. Struct.* **2016**, *111*, 80–92. [CrossRef]
19. Li, S.; Shan, S.D.; Zhai, C.H.; Xie, L.L. Experimental and numerical study on progressive collapse process of RC frames with full-height infill walls. *Eng. Fail. Anal.* **2016**, *59*, 57–68. [CrossRef]
20. Qian, K.; Li, Y.; Yang, T.; Li, B. Progressive collapse resistance of posttensioned concrete beam-column subassemblages with unbonded posttensioning strands. *J. Struct. Eng.* **2018**, *144*, 04017182. [CrossRef]
21. Adam, J.M.; Parisi, F.; Sagaseta, J.; Lu, X.Z. Research and practice on progressive collapse and robustness of building structures in the 21st century. *Eng. Struct.* **2018**, *173*, 122–149. [CrossRef]
22. Crawford, J.E. *Retrofit Methods to Mitigate Progressive Collapse; National Workshop and Recommendations for Future Effort*; The Multihazard Mitigation Council of the National Institute of Building Sciences: Rosemont, IL, USA, 2002.

23. Hayes, J.R.; Woodson, S.C.; Pekelnicky, R.G.; Poland, C.D.; Corley, W.G.; Sozen, M. Can strengthening for earthquake improve blast and progressive collapse resistance. *J. Struct. Eng.* **2005**, *131*, 1157–1177. [CrossRef]
24. Galal, K.; El-Sawy, T. Effect of retrofit strategies on mitigating progressive collapse of steel frame structures. *J. Constr. Steel Res.* **2010**, *66*, 520–531. [CrossRef]
25. Liu, J.L. Preventing progressive collapse trough strengthening beam-to-column connection, Part 1: Theoretical analysis. *J. Constr. Steel Res.* **2010**, *66*, 229–237. [CrossRef]
26. Liu, J.L. Preventing progressive collapse trough strengthening beam-to-column connection, Part 2: Finite element analysis. *J. Constr. Steel Res.* **2010**, *66*, 238–247. [CrossRef]
27. Chen, J.L.; Peng, W.B.; Ma, R.L.; He, M.J. Strengthening of horizontal bracing on progressive collapse resistance of multistory steel moment frame. *J. Perform. Constr. Facil.* **2012**, *26*, 720–724. [CrossRef]
28. Tsai, M.H. A performance-based design approach for retrofitting regular building frames with steel braces against sudden column loss. *J. Constr. Steel Res.* **2012**, *77*, 1–11. [CrossRef]
29. Kim, J.; Shin, W.S. Retrofit of RC frames against progressive collapse using prestressing tendons. *Struct. Des. Tall. Spec.* **2013**, *22*, 349–361. [CrossRef]
30. Naderi, D.; Adaros, M.S.; Wood, S. *Use of Ring Beams for Progressive Collapse Retrofit*; ASCE Structures Congress: Portland, OR, USA, 2015.
31. Adaros, M.S.; Smilowitz, R. Challenges and considerations for retrofit of existing structures for progressive collapse. *J. Perform. Constr. Facil.* **2015**, *29*, B4014001. [CrossRef]
32. Alrudaini, T.M.S. A New Mitigation Scheme to Resist the Progressive Collapse of Reinforced Concrete Buildings. Ph.D. Thesis, University of Wollongong, Wollongong, Australia, 2011.
33. Galli, R.M.; El-Domiaty, K.; Wolff, E. *Applicability of FRP System for Retrofitting Existing Buildings to Resist Progressive Collapse*; ASCE Structures Congress: Chicago, IL, USA, 2012.
34. Wang, D.; Wang, Z.; Yu, T.; Li, H. Seismic performance of CFRP-retrofitted large-scale rectangular RC columns under lateral loading in different directions. *Compos. Struct.* **2018**, *192*, 475–488. [CrossRef]
35. Chen, W.H.; Shou, W.R.; Qiao, Z.H.; Cui, S.S. Seismic performance of non-ductile RC frames strengthened with CFRP. *Compos. Struct.* **2019**, *221*, 110870. [CrossRef]
36. Orton, S.L. Development of a CFRP System to Provide Continuity in Existing Reinforced Concrete Buildings Vulnerable to Progressive Collapse. Ph.D. Thesis, The University of Texas at Austin, Austin, TX, USA, 2007.
37. Qian, K.; Li, B. Strengthening and retrofitting of RC flat slabs to mitigate progressive collapse by externally bonded CFRP laminates. *J. Compos. Constr.* **2013**, *17*, 554–565. [CrossRef]
38. Qian, K.; Li, B. Strengthening of multibay reinforced concrete flat slabs to mitigate progressive collapse. *J. Struct. Eng.* **2015**, *141*, 04014107. [CrossRef]
39. Feng, P.; Shi, K.X.; Qin, W.H.; Ou, X. Experimental study on progressive collapse behavior of GFRP strengthened RC beam-column structures. *Ind. Constr.* **2013**, *43*, 64–68. (In Chinese)
40. Qin, H.W.; Feng, P.; Shi, K.J.; Su, Y. Numerical analysis of progressive collapse behavior of glass fiber reinforced polymer strengthened beam-column structures. *J. Tongji Univ. Nat. Sci.* **2014**, *42*, 1647–1653. (In Chinese)
41. Liu, T.; Xiao, Y.; Yang, J.; Chen, B.S. CFRP strip cable retrofit of RC frame for collapse resistance. *J. Compos. Constr.* **2017**, *21*, 04016067. [CrossRef]
42. GB50011-2010. *Code for Seismic Design of Building*; Ministry of Housing and Urban Rural Development: Beijing, China, 2010. (In Chinese)
43. GB50010-2010. *Code for Design of Concrete Structures*; Ministry of Housing and Urban Rural Development: Beijing, China, 2015. (In Chinese)
44. Open System for Earthquake Engineering Simulation (OpenSees). 2019. Available online: http://opensees.berkeley.edu/wiki/index.php/Command_Manual (accessed on 6 January 2019).
45. Spacone, E. Flexibility-Based Finiteelement Models for the Nonlinear Static and Dynamic Analysis of Concrete Frame Structures. Ph.D. Thesis, University of California, Berkeley, CA, USA, 1994.
46. Wang, Z.Y.; Wang, D.Y.; Smith, S.T.; Lu, D.G. CFRP-confined square RC columns. II: Cyclic axial compression stress-strain model. *J. Compos. Constr.* **2012**, *16*, 161–170. [CrossRef]
47. GB50367-2013. *Code for Design of Strengthening Concrete Structures*; Ministry of Housing and Urban Rural Development: Beijing, China, 2013. (In Chinese)

48. Zhang, J.T. Collapse-Based Retrofit and Optimal Design Method of Viscous Dampers. Master's Thesis, Harbin Institute of Tecnology, Harbin, China, 2019.
49. FEMA. *Seismic Performance Assessment of Buildings*; Methodology; Applied Technology Council: Redwood, CA, USA, 2012.